Low-Loss Twists in Oversized Rectangular Waveguide

JOHN L. DOANE, SENIOR MEMBER, IEEE

Abstract —Twists may be required in oversized rectangular waveguide used for low-loss transmission at the higher microwave and millimeter-wave frequencies. The unwanted mode conversion in such twists is calculated here from numerical integration of the coupled mode equations, considering simultaneous coupling of the five lowest order modes coupled in a twist. Twists with tapered or linearly varying rates of twist are shown to be superior in medium- or broad-band applications to those with uniform twist rate, such as those normally made commercially for single-mode waveguide. Some recent applications and designs for oversized rectangular waveguides are presented in [1].

Measurements consistent with these theoretical calculations are discussed for uniform twists in WR90 (0.9×0.4 in.) at 60 GHz and for an electroformed twist having a linearly tapered rate of twist in WR187 (1.872×0.872 in.) from 15.7 to 17.7 GHz.

The coupling coefficients needed in the calculations are derived in an appendix, and are compared with the results of other work, including a modal expansion of the dominant mode in twisted waveguide. A second appendix considers the transmission through an oversized waveguide with a mode converter generating a trapped unwanted mode, and derives the result for the dependence of the resonance depth on the mode conversion and the attenuation of the trapped mode.

I. INTRODUCTION

OVERSIZED (overmoded) waveguide has been used occasionally for many years to reduce the ohmic (wall) losses of smaller dominant-mode waveguide. At millimeter wavelengths, oversized waveguide is also required to avoid breakdown when high power is transmitted. Rectangular oversized waveguide is often convenient, particularly when the transmitter and receiver are also in rectangular waveguide. Some recent applications and designs for oversized rectangular waveguides are presented in [1].

Twists in oversized rectangular waveguide can be used not only for the same reasons as in regular sized waveguide, but also to avoid negotiating an unfavorable bend. For electrical and sometimes for mechanical fabrication reasons, overmoded waveguide bends in the plane of the broad wall should be avoided [1]. When the electric field is oriented in the usual way, such bends are called H plane bends, but if the electric field is oriented parallel to the broad wall ("tall guide" configuration), these would be E plane bends (see Fig. 1). Geometrically, the combination of a favorable bend (in the plane of the narrow wall) and a twist can replace an unfavorable bend.

Bends in the plane of the broad wall are unfavorable because of the closeness of the most strongly generated unwanted mode to the mode of propagation (see Fig. 2).

Much longer bends are required to reduce the net coupling to nearby modes which have phase velocities close to that of the desired mode [1]. The coupling changes sign each time the difference in phase of the desired and undesired modes changes sign. In the ordinary electric field configuration, the propagating TE_{10} mode is coupled to TE_{20} (and to TE_{m0} where m is even) in an unfavorable H plane bend, but to the more distant TE_{11}/TM_{11} (and to TE_{1m}/TM_{1m} where m is odd) in an E plane bend [2]. The difference in mode conversion in the two types of bends is even more pronounced in the tall guide configuration where TE_{01} is propagated. There, a (favorable) H plane bend couples TE_{01} to TE_{02} which, in rectangular waveguide with a 2:1 aspect ratio, is as far away as TE_{40}. On the other hand, an E plane bend is very undesirable because it couples TE_{01} to the nearby TE_{11}/TM_{11} pair.

The tall guide configuration is often desirable because the ohmic wall losses reasonably far above cutoff are inversely proportional to the length of the wall parallel to the electric field. An added advantage is the relatively benign behavior of H plane bends in tall guide. The TE_{02} mode may even be cut off, which would allow very compact H plane bends. In the ordinary configuration, the TE_{11}/TM_{11} pair coupled by E plane bends would be much closer to the propagating mode and almost certainly would not be cut off in an overmoded application.

Twists in overmoded rectangular waveguide cause coupling between modes separated by an odd integer in both indices. To design a twist when propagating TE_{10}, it is usually sufficient to consider coupling only to TE_{01}, since other coupled modes are further away (Fig. 2(b)). However, in the tall guide case when TE_{01} is the desired propagating mode, the coupled TE_{21}, TM_{21}, and TE_{30} modes may be about as close to TE_{01} as TE_{10} is. Hence, one may have to consider simultaneous pairwise coupling between all these modes.

When the change in twist angle θ along the waveguide longitudinal axis is not too rapid in a wavelength ($d\theta/dz \ll 1/\lambda$), the coupling between modes is linear in $d\theta/dz$. The proportionality constant is called the coupling coefficient, which depends on the relative waveguide dimensions

Manuscript received September 3, 1987; revised December 24, 1987. This work was supported by the U.S. Department of Energy under Contract DE-AC02-76CH03073.

The author is with the Princeton Plasma Physics Laboratory, Princeton, NJ 08544.

IEEE Log Number 8820440.

0018-9480/88/0600-1033$01.00 ©1988 IEEE

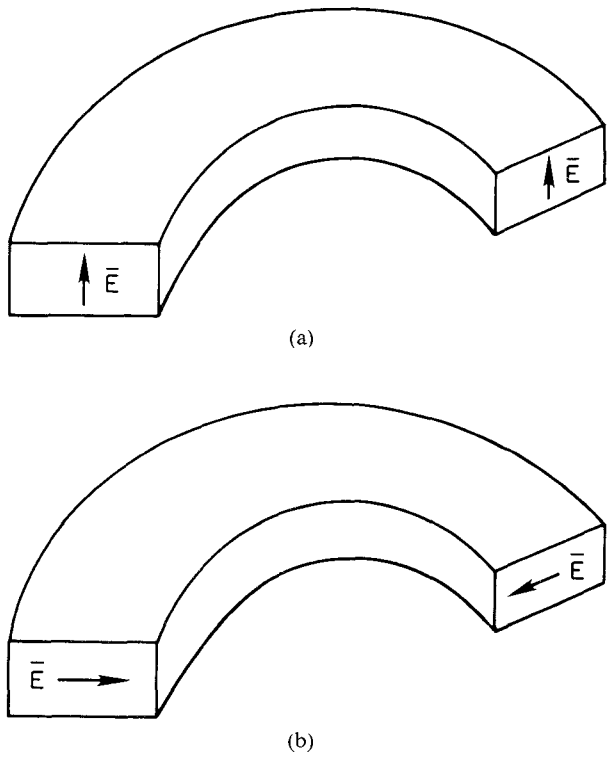

Fig. 1. Unfavorable bend geometries in oversized rectangular waveguide. (a) TE_{10} H plane bend. (b) TE_{01} ("tall guide") E plane bend

(aspect ratio) and the mode indices. Katsenelenbaum [3] calculated the TE_{10}/TE_{01} coupling coefficient and showed that reasonably far above cutoff of both modes it was almost independent of frequency. Marhic [4], with infrared applications such as CO_2 lasers in view, derived the coupling coefficients for all modes coupled by twists in the case where these modes are very far above cutoff.

We derive in Appendix I expressions for all the twist coupling coefficients without the restriction that the coupled modes are far above cutoff. The derivation adopts the approach used in [5] and [6] for deriving the coupling coefficients due to small wall deformations in circular waveguide. The derivation is valid except in a case where the two coupled modes are degenerate (have the same propagation constant), such as would occur in square waveguide with TE_{10} and TE_{01}.

The results of these derivations are mostly in agreement with Marhic [4]. We find, however, that the coupling between two TM modes can be nonzero, in disagreement with the result of [4]. Further, a $\sqrt{2}$ normalization factor for modes with a zero index is missing from the coupling coefficients in [4]. With this normalization factor present, our result for TE_{10}–TE_{01} coupling agrees with Katsenelenbaum [3].

At the end of Appendix I we also show how our derivation of the coupling coefficients for the TE_{10} mode is equivalent to the modal expansion of the dominant hybrid mode satisfying the boundary conditions in uniformly twisted waveguide [7]. Results similar to those in [7] have also been obtained recently without the restriction of small coupling [8].

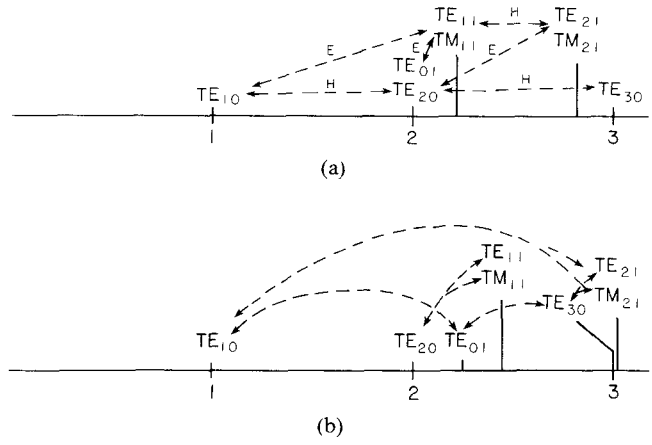

Fig. 2. Normalized cutoff frequencies in oversized rectangular waveguides. (a) $a/b = 2$. (b) $a/b = 2.25$ (as in WR90). Arrows show modes coupled by E and H plane bends, respectively (in Fig. 2 (a)), and by twists (Fig. 2 (b)).

In Section II we present some examples of the mode conversion in twists calculated using the coupling coefficients from Appendix I together with numerical solution of the coupled mode equations. Except in narrow-band applications where TE_{10} is propagated, twists with a varying (nonconstant) rate of twist change $d\theta/dz$ are generally preferable to those with constant $d\theta/dz$. The latter type of twist is generally produced by ordinary waveguide twisting methods. In Section III we discuss the fabrication and measurement of twists of both types. We compare the results of the measurements with predictions from Section II and also Appendix II, which shows how the transmission through an overmoded waveguide with a single mode converter is determined by the mode conversion and the ohmic attenuation of the (trapped) unwanted mode.

II. Examples of Mode Conversion in Twists: Theory

For oversized waveguides that can propagate several modes $m = 1$ to N with phase propagation constants β_m, the coupled mode equations for twists with twist angle $\theta(z)$ can be written (See Appendix I, eq. (A7)):

$$dA_m/dz = \sum_{\substack{n=1 \\ n \neq m}}^{N} \kappa_{mn}(d\theta/dz)\exp(j\Delta\beta_{mn}z)A_n \qquad (1)$$

where

$$\Delta\beta_{mn} = \beta_m - \beta_n \qquad (2)$$

and the A_m are the mode amplitudes. Normally the attenuations $\alpha_m L$ over the length L of the twist are negligible, and these are accordingly neglected in (1). In Appendix I, formulas are derived for the coupling factors K_{mn}, where

$$K_{mn} = \kappa_{mn}\, d\theta/dz. \qquad (3)$$

The coupling coefficients κ_{mn} in (1) are dimensionless. Far above cutoff, these coefficients approach limiting values. According to the formulas derived in Appendix I, some of these values depend somewhat on the waveguide aspect ratio a/b. For $a/b = 2.25$, as in WR90, Table I

TABLE I
COUPLING COEFFICIENTS κ_{mn} FAR ABOVE CUTOFF ($a/b = 2.25$)

	TE_{10}	TE_{01}	TE_{30}	TE_{21}	TM_{21}
TE_{10}	0	0.811	0	−0.130	0.428
TE_{01}	−0.811	0	−0.270	0	0
TE_{30}	0	+0.270	0	1.331	0.463
TE_{21}	+0.130	0	−1.331	0	0
TM_{21}	−0.428	0	−0.463	0	0

lists the limiting values far above cutoff for the lowest modes coupled to TE_{10} and TE_{01}.

Note from the table that

$$\kappa_{mn} = -\kappa_{nm} \tag{4}$$

as is required for power conservation. Also, the coupling is zero unless the first and second indices of the coupled modes both differ by an odd number.

By far the easiest twist angle variation to fabricate is

$$d\theta/dz = \theta_{\text{tot}}/L \tag{5}$$

where θ_{tot} is the total twist angle. The variation in (5) describes quite well most commercial twists. For this case, eqs. (1) have a closed-form solution. When there is only one important unwanted mode n, with zero amplitude at the beginning of the twist (where $A_1(0) = 1$), the solution for the fractional unwanted mode power at the end of the twist is [9]

$$|A_n(L)|^2 = (\kappa_{1n}\theta_{\text{tot}})^2\left(\frac{\sin u}{u}\right)^2 \tag{6a}$$

where

$$u \equiv \left[(\Delta\beta_{1n}L/2)^2 + (\kappa_{1n}\theta_{\text{tot}})^2\right]^{1/2}. \tag{6b}$$

The oscillatory nature predicted by (6) for the spurious mode power as a function of overall twist length L shows up clearly in Fig. 3. The spurious mode levels shown in these and the following figures were calculated by simultaneous numerical integration of (1) with $N = 5$. Notice from Fig. 3(a) that low mode conversion at 60 GHz can be achieved with constant rate of twist for twist length as short as $L = 7$ in. and also for L near 15 or 16 in.

If TE_{01} ("tall guide" mode) is propagated in WR90 instead of TE_{10}, however, the mode conversion near $L = 7$ in. may be unacceptable, as Fig. 3(b) shows. The difficulty is that TE_{01} couples directly to TE_{30} as well as to TE_{10}. Furthermore, TE_{30}, TE_{21}, and TM_{21} are all closer to TE_{01} (smaller $\Delta\beta$) than to TE_{10}.

Since $\Delta\beta$ varies with frequency, the mode conversion in twists with constant $d\theta/dz$ will also oscillate with frequency. This behavior is shown in Fig. 4. For any two modes m and n far above cutoff $\Delta\beta_{mn}$ continually decreases with increased frequency as $1/f$. Consequently, both the period and the maximum in the mode conversion oscillations get larger as the frequency increases (see Fig. 4 and (6)).

Fortunately, by using a nonconstant variation in $d\theta/dz$, the average mode conversion may be reduced substantially, as shown in Figs. 4 and 5. The linearly varying, or "triangular," rate of twist variation is quite effective, especially over large bandwidths. This variation is described by

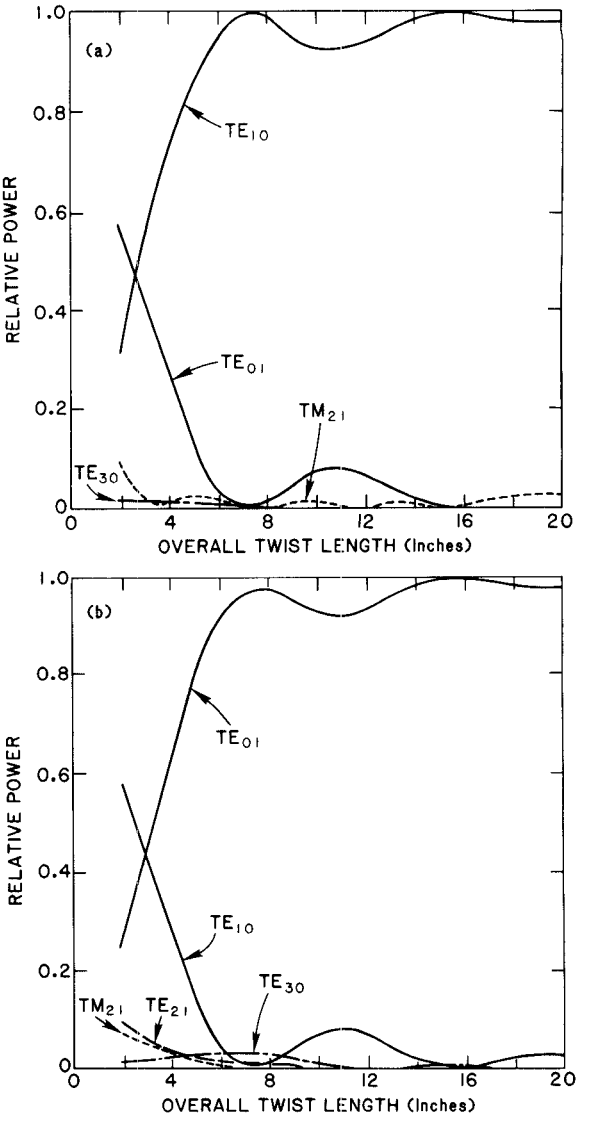

Fig. 3. Relative mode levels at 60 GHz at the end of 90° twists in WR90 (0.9×0.4 in. ID) with a constant rate of change of twist angle. (a) TE_{10} incident. (b) TE_{01} incident.

$$d\theta/dz = \begin{cases} 4\theta_{\text{tot}}z/L^2, & 0 \leqslant z \leqslant L/2 \\ 4\theta_{\text{tot}}(L-z)/L^2, & \dfrac{L}{2} \leqslant z \leqslant L. \end{cases} \tag{7}$$

The maximum rate of twist, at $z = L/2$, is double that in the constant rate of twist case.

Other variations in $d\theta/dz$ such as cosine, cosine-squared, or hyperbolic secant also give lower average mode conversions than the constant $d\theta/dz$ twist. These functional forms have been useful as curvature variations and also as ellipticity variations in certain applications involving low mode conversion bends [10] and polarization converters [11] in oversized waveguide. For the twist examples considered here, however, the "triangular" variation in $d\theta/dz$ appears the best.

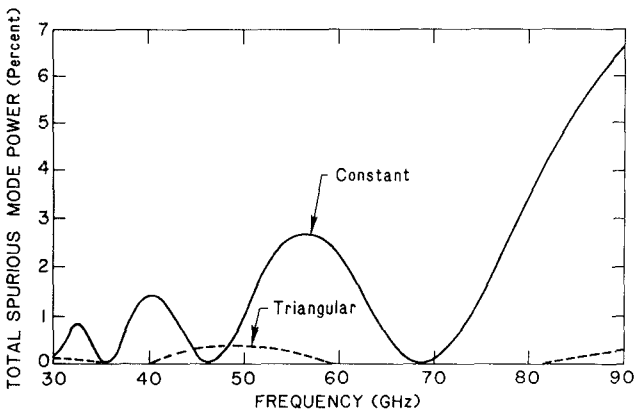

Fig. 4. Mode conversion in 18 in. 90° WR90 twists propagating TE_{10} with constant or linearly varying ("triangular") rates of twist.

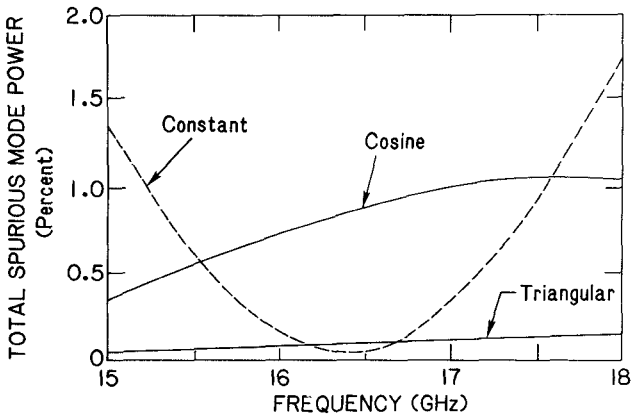

Fig. 5. Mode conversion in 20 in. 90° twists in WR187 (1.872×0.872 in. ID) propagating TE_{01} for various rates of twist.

The twist with triangular $d\theta/dz$ whose theoretical performance is shown in Fig. 4 was designed for a broad-band 30 to 90 GHz WR90 waveguide transmission system to carry signals over 100 ft to and from a tokamak fusion device for plasma diagnostics applications. WR187 (Fig. 5) is used to transmit signals from 15.7 to 17.7 GHz for new FAA airport surveillance radars. In both of these cases, twists may be used to avoid the unfavorable bend geometries shown in Fig. 1.

For narrow-band applications using TE_{10}, short twists with constant $d\theta/dz$ can be acceptable. Fig. 6 shows the predicted mode conversion from 50 to 70 GHz for such twists. For the 7.25 in. twist, the difference between the spurious TE_{01} and the total spurious mode power is mainly due to TM_{21}, while for the 13.25 in. twist, less than 1/2 percent of the power is in TM_{21}. Measurements on twists with these lengths are discussed in the next section.

III. Mode Conversion in Twists: Experiments

The twists corresponding to Fig. 6 were measured with the setup shown schematically in Fig. 7. As discussed in Appendix II, the presence of spurious modes shows up as resonances as the frequency is swept. The depth of the resonances depends not only on the mode conversion in the twist, but also on the spurious mode attenuation.

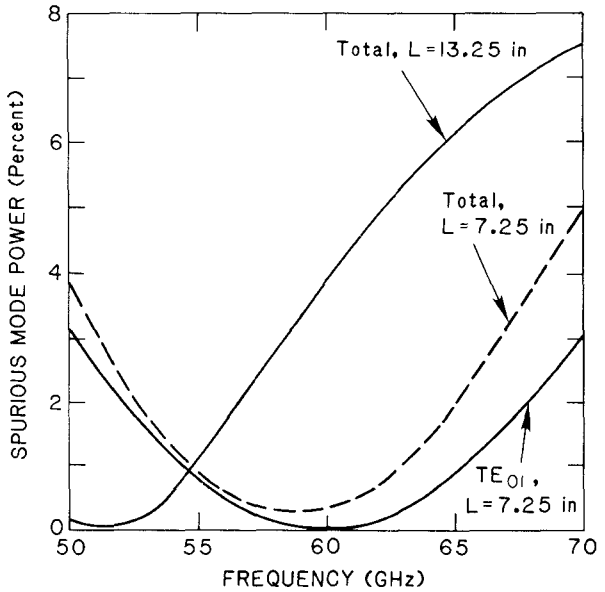

Fig. 6. Mode conversion in 7.25 in. and 13.25 in. 90° twists in WR90 with constant rate of twist. Almost all the spurious mode power for the 13.25 in. twist is in TE_{01}.

When there was no twist in the setup of Fig. 7, no trapped mode resonances were seen, indicating that the mode conversion in the 12 in. (linear) tapers was completely negligible.

For calibration purposes, the flanges at the junction of two WR90 waveguide sections were twisted by 5°. The overall length of the two sections was 12 in.; the resulting "calibrated mode converter" was inserted as the twist of Fig. 7. Theoretically, the mode conversion from TE_{10} to TE_{01} at such an abrupt twist is $K_0\Delta\theta$, where $K_0 \simeq 8/\pi^2$ (see Table I and (A18)). The TE_{01} spurious mode power ($|T_2|^2$ in the notation of Appendix II) should then be $(K_0\Delta\theta)^2 \simeq 0.005$, or about 23 dB below the power in TE_{10}. The coupling coefficient from TE_{10} to TM_{21} is 0.44 at 60 GHz; the level of TM_{21} (the next most strongly coupled mode) should be about 0.0015, or 28 dB below TE_{10}.

Since both TM_{21} and TE_{01} are generated in the calibrated twist, we would expect to see resonances with two different depths, with some interaction where the resonances coincide. The resonances occur at spacings corresponding to changes of π in $\beta_2 L$, where β_2 is the spurious mode propagation constant, and L is about 6 ft (see Fig. 7). The observed resonances are spaced closer than 100 MHz and vary rapidly between 2 and 10 percent in depth over the entire band from 50 to 70 GHz. This result is reasonably consistent with the 1:3 ratio in the TM_{21} to TE_{01} power levels.

The resonance depths for the 7.25 in. twist were somewhat more uniform at between 3 to 6 percent near 60 GHz, and increased to almost 20 percent near 50 or 70 GHz. This result is in qualitative agreement with Fig. 6. The resonances are not, however, quite as deep as would be expected from comparison of the resonances of the "calibrated twist."

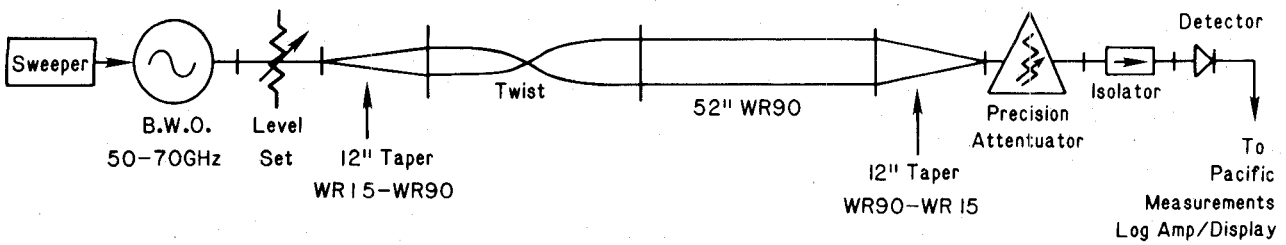

Fig. 7. Schematic of measurement apparatus used to check the mode conversion in the twists corresponding to Fig. 6.

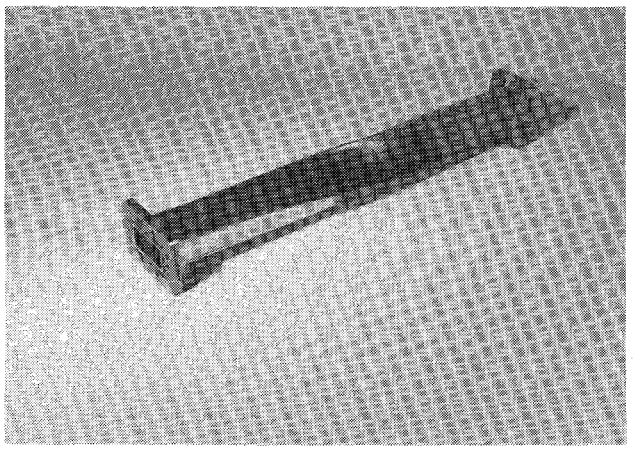

Fig. 8. Electroformed 90° WR187 twist with a "triangular" variation in the twist rate over a 20 in. region.

The resonance depths for the 13.25 in. twist were less than 2 percent near 50 GHz, and increased gradually to 25 percent at 60 GHz. This result also agrees qualitatively with Fig. 6. Above 59 GHz, however, particularly between 59 and 63 GHz, the main resonance depths vary periodically with a period of about 600 MHz; smaller resonances also appear interleaved with the main ones. The maximum resonance depth in this region is about 40 percent near 62 to 63 GHz. From 63 to 70 GHz the depth is 20 to 30 percent.

Both of these twists were fabricated by filling straight lengths of WR90 with sand to minimize the cross-sectional distortion during twist. (The broad walls in the center of the 7.25 in. twist curved in slightly, reducing the waveguide b dimension by a maximum of 1/32 in.) A jig was also constructed to prevent the waveguide centerline from moving during twisting. The overall waveguide lengths were 10 and 18 in., respectively, for the cases where the twisted regions were nominally 7.25 and 13.25 in. Regardless of the overall length, it was not possible to make the twisted region in a WR90 90° twist extend longer than about 13 in. with the simple technique of fixing one waveguide end and twisting the other.

Mechanical measurements on the "7.25-in." twist showed a very nearly uniform 12.5°/in. rate of twist over the central 6 3/4 in. span, accounting for about 84° of the total. The rate of twist tapered to zero gradually for about 3/4 in. on each end beyond this.

By comparison, the beat wavelengths $2\pi/\Delta\beta$ for TE_{10} to TE_{01} and TE_{10} to TM_{21} are 8 in. and 4 in. at 60 GHz, respectively. Hence, the 3/4 in. taper lengths on either end of the twist are not long enough to be completely effective (about one half beat wavelength is required); nevertheless, the effect will be to modify the behavior of a constant rate of twist to have mode conversion more like that of the "triangular," or linearly tapered, rate of twist. From the behavior of the two types of twists shown in Fig. 4 (see the region 40–50 GHz in particular), we can see that the effect is to eliminate the sharp null in the mode conversion while decreasing the maximum in the mode conversion for the constant rate of twist. This effect appears to be confirmed in our measurements of the 7.25 in. twist.

Mechanical measurements on the 13.25 in. twist also showed the presence of tapers in the rate of twist at each end. These tapers, however, only extended about 1/4 in. on each end; the uniformly twisted region accounted for about 88° of the total.

The WR187 twist shown in Fig. 8 was electroformed using an aluminum mandrel machined on a numerically controlled 4-axis milling machine. The rate of twist has the "triangular" form described by (7), where the twisted region has length $L = 20$ in. Transmission measurements of this twist between two tapers to fundamental waveguide (WR62) showed resonances about 0.1 dB (2 percent) deep from 15.7 to 17.7 GHz; the resonances due to mode conversion in the tapers alone (without the twist) were less than 1 percent deep. These tapers also changed the polarization so that the electric field in the WR187 waveguide was parallel to the broad wall; that is, TE_{01} was propagated through the twist. Considering that the ohmic loss $\alpha_2 L$ of the unwanted trapped mode (TE_{10}) in this twist and the tapers must be quite small, we conclude from these measurements that the unwanted mode power $|T_2|^2$ must be very small indeed (see (A54). This result is consistent with Fig. 5.

IV. Conclusions

Expressions have been derived for the coupling between modes in twisted oversized (overmoded) rectangular waveguides. The coupled mode equations involving these expressions have been numerically integrated for several cases of constant and tapered rates of twist. In this manner, linear tapering of the twist rate was shown theoretically to reduce the mode conversion in broad-band applications. Twists have been fabricated to avoid unfavorable bends in oversized waveguide runs for airport radar and plasma diagnostics applications. With reference to a discrete abrupt twist and also to the derived characteristics of resonance losses in transmission measurements, measurements on

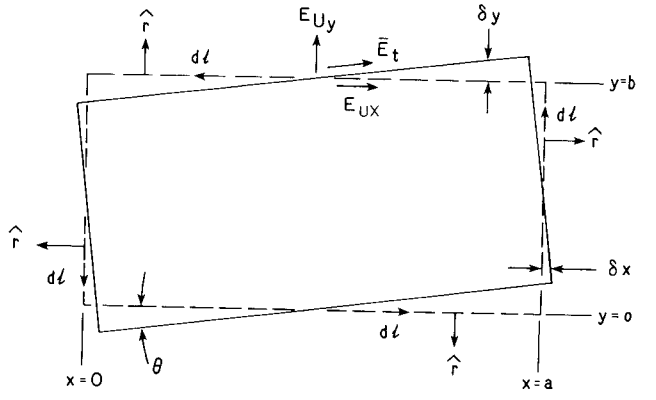

Fig. 9. Geometry for the integration around a twisted waveguide wall to determine the coupling coefficients.

these twists were shown to agree qualitatively with the predictions from the coupled wave equations.

Appendix I
Coupling Coefficients for Rectangular Waveguide Twists

To find the coupling coefficients between modes due to twists in rectangular waveguide, first write the total fields $\boldsymbol{E}$ and $\boldsymbol{H}$ in terms of the normal mode fields $\boldsymbol{e}_m$ and $\boldsymbol{h}_m$:

$$\boldsymbol{E} = \sum_m A_m^+(z) e^{-j\beta_m z} \boldsymbol{e}_m^+ + \sum_m A_m^-(z) e^{+j\beta_m z} \boldsymbol{e}_m^- \quad \text{(A1)}$$

and similarly for $\boldsymbol{H}$. Here $A_m^+(z)$ and $A_m^-(z)$ are the amplitudes of the forward and backward traveling mth mode, respectively. The β_m are the propagation constants, and any attenuation constants α_m due to ohmic loss on the waveguide wall can be included in the $A_m^\pm$ through the exponential factors $e^{\mp \alpha_m z}$. The normal mode fields themselves are orthonormal and independent of z:

$$\iint \left[\boldsymbol{e}_m^+ \times (\boldsymbol{h}_n^\pm)^*\right] \cdot d\boldsymbol{S} = \pm \delta_{mn} \quad \text{(A2)}$$

where S is the waveguide cross section.

Following Carlin and Moorthy [5] (see also [6]), we may apply certain vector identities and (A2) with the result

$$\frac{d}{dz} A_m^\pm(z) = \mp \frac{1}{2} e^{\pm j\beta_m z} \cdot \oint \left[\boldsymbol{E}_D \times (\boldsymbol{h}_m^\pm)^* + (\boldsymbol{e}_m^\pm)^* \times \boldsymbol{H}_D\right] \cdot \hat{r}\, dl \quad \text{(A3)}$$

where the integral is taken around the circumference of the cross section, and $\hat{r}$ is the unit vector perpendicular to the waveguide wall and directed outward. Here we have also written the total fields E and H in terms of the total fields $\boldsymbol{E}_u$ and $\boldsymbol{H}_u$ in the undeformed waveguide plus those arising from any deformations (with subscript D):

$$\boldsymbol{E} = \boldsymbol{E}_u + \boldsymbol{E}_D \quad \text{(A4)}$$

and similarly for $\boldsymbol{H}$. Equation (A3) is rather general, valid for rather arbitrary waveguide cross sections and (lossless) wall reactances. In smooth waveguide, the second cross product on the right-hand side of (A3) vanishes, because the tangential fields $\boldsymbol{e}_m \times \hat{r}$ must vanish on the wall.

The fields $\boldsymbol{E}_D$ due to wall deformations in (A3) can be related to the fields $\boldsymbol{E}_u$ in undeformed rectangular waveguide by requiring that the total field tangential to the deformed wall $\boldsymbol{E}_t$ must vanish. To first order in the wall deformations δx and δy, we obtain (see Fig. 9)

$$E_{Dx} = -\delta y \frac{\partial E_{ux}}{\partial y} - E_{uy} \frac{\partial \delta y}{\partial x}, \qquad \hat{r} = \pm \hat{y} \quad \text{(A5a)}$$

$$E_{Dy} = -\delta x \frac{\partial E_{uy}}{\partial x} - E_{ux} \frac{\partial \delta x}{\partial y}, \qquad \hat{r} = \pm \hat{x} \quad \text{(A5b)}$$

$$E_{Dz} = -\delta y \frac{\partial E_{uz}}{\partial y} - E_{uy} \frac{\partial \delta y}{\partial z}, \qquad \hat{r} = \pm \hat{y} \quad \text{(A6a)}$$

$$E_{Dz} = -\delta x \frac{\delta E_{uz}}{\partial x} - E_{ux} \frac{\partial \delta x}{\partial z}, \qquad \hat{r} = \pm \hat{x}. \quad \text{(A6b)}$$

The field components in undeformed waveguide can in turn be written in terms of the components of the normal mode fields $\boldsymbol{e}_n$ through the sum in (A1). Backscattering into oppositely traveling modes $\boldsymbol{e}_n$ can generally be neglected if the wall deformations vary slowly in a free-space wavelength. Then from (A3), (A5), and (A6), the coupling between forward traveling modes takes the form

$$\frac{dA_m}{dz} = \sum_n K_{mn} e^{j\Delta\beta_{mn} z} A_n \quad \text{(A7)}$$

where

$$\Delta\beta_{mn} = \beta_m - \beta_n \quad \text{(A8)}$$

and we have dropped the + superscripts.

The coupling factors K_{mn} contain integrals around the circumference of the waveguide derived from the right-hand side of (A3). Using (A5), (A6), and (A7), and noting that dl changes sign on opposite sides of the waveguide (Fig. 9),

$$K_{mn} = \tfrac{1}{2} \int_0^a dx \left[T_x(y=b) - T_x(y=0)\right] + \tfrac{1}{2} \int_0^b dy \left[T_y(x=a) - T_y(x=0)\right] \quad \text{(A9)}$$

where

$$T_x = \left[\delta y \left(\frac{\partial e_{nx}}{\partial y}\right) + e_{ny} \left(\frac{\partial \delta y}{\partial x}\right)\right] h_{mz} + \delta y \left[\left(\frac{\partial e_{nz}}{\partial y}\right) - j\Delta\beta_{mn} e_{ny}\right] h_{mx} \quad \text{(A10a)}$$

and

$$T_y = \left[\delta x \left(\frac{\partial e_{ny}}{\partial x}\right) + e_{nx} \left(\frac{\partial \delta x}{\partial y}\right)\right] h_{mz} + \delta x \left[\frac{\partial e_{nz}}{\partial x} - j\Delta\beta_{mn} e_{nx}\right] h_{my}. \quad \text{(A10b)}$$

The derivatives of δx and δy with respect to z in (A6) have been eliminated by using the following equation, which is valid for coupling between modes with different propagation constants β [12]:

$$\frac{\partial}{\partial z} \leftrightarrow -j\Delta\beta_{mn}. \quad \text{(A11)}$$

The coupling factors from (A7), (A9), and (A10) are still quite general, and can be used for E and H plane bends as well as for twists. By replacing $\beta_m z$ by $\int \beta_m \, dz$ everywhere, the coupling in smooth rectangular waveguide tapers can also be handled with these equations.

For rectangular waveguide twists, we have (see Fig. 9)

$$\delta y = \left(x - \frac{a}{2}\right)\theta \qquad \frac{\partial \delta y}{\partial x} = \theta \qquad \text{on } y = 0, b \quad \text{(A12a)}$$

$$\delta x = \left(\frac{b}{2} - y\right)\theta \qquad \frac{\partial \delta x}{\partial y} = -\theta \qquad \text{on } x = 0, a. \quad \text{(A12b)}$$

Substituting these expressions into (A10) along with the expression for the fields of normal modes carrying unit power, we can obtain from (A9) the coupling factors.

Here we define

$$P_m \equiv \beta_m / k \qquad k = 2\pi/\lambda = 2\pi f/c \quad \text{(A13)}$$

$$R \equiv a/b \quad \text{(A14)}$$

and

$$\theta' = d\theta/dz. \quad \text{(A15)}$$

The modes are coupled by the change in the twist angle rather than by the twist angle θ itself, since if θ were constant we could always rotate the coordinate system to make $\theta = 0$ again. Hence we have made use of the equivalence in (A11) again to write the following coupling factors in terms of θ' instead of θ.

In general, there is no coupling between modes due to twist unless the modes have opposite parity in both indices. That is, in the following,

$$K_{mn} \neq 0 \text{ only if } p + r \text{ and } q + s \text{ are both odd.} \quad \text{(A16)}$$

For coupling from $\mathrm{TE}_{pq}(m)$ to $\mathrm{TE}_{rs}(n)$, we have, when (A16) is satisfied,

$$K_{mn} = -(K_0/D)(P_m + P_n)(N_1 + N_2 N_3)\theta' \quad \text{(A17)}$$

where

$$K_0 = (8/\pi^2) \quad \text{(A18)}$$

$$D \equiv (P_m P_n \epsilon_m \epsilon_n)^{1/2} R(r^2 - p^2)^2 (s^2 - q^2)^2 \cdot (p^2 + R^2 q^2)^{1/2} (r^2 + R^2 s^2)^{1/2} \quad \text{(A19)}$$

$$N_1 = (p^2 + R^2 q^2)(r^2 + R^2 s^2)(q^2 r^2 - p^2 s^2) \quad \text{(A20a)}$$

$$N_2 = r^2 s^2 - p^2 q^2 \quad \text{(A20b)}$$

$$N_3 = p^2 r^2 - R^4 q^2 s^2 + R^2(p^2 s^2 - q^2 r^2) \cdot [(P_m - P_n)/(P_m + P_n)] \quad \text{(A20c)}$$

$$\epsilon_m = \begin{cases} 2 & \text{if } p \text{ or } q = 0 \\ 1 & \text{otherwise} \end{cases} \quad \text{(A21)}$$

and similarly for ϵ_n.

For coupling between $\mathrm{TM}_{pq}(m)$ and $\mathrm{TM}_{rs}(n)$,

$$K_{mn} = 2(K_0/D)\, pqrs N_4 N_5 \theta' \quad \text{(A22)}$$

where

$$N_4 = P_n(p^2 + R^2 q^2) + P_m(r^2 + R^2 s^2) \quad \text{(A23a)}$$

and

$$N_5 = R^2(s^2 - q^2) - (r^2 - p^2). \quad \text{(A23b)}$$

Finally, for coupling between $\mathrm{TE}_{pq}(m)$ and $\mathrm{TM}_{rs}(n)$,

$$K_{mn} = 2(K_0/D)\, Rrs\left[R^2 p^2 (s^2 - q^2)^2 + q^2 (r^2 - p^2)^2\right]\theta'. \quad \text{(A24)}$$

Notice that the coupling factors K_{mn} in (A17) and (A22) change sign under interchange of modes: $m \leftrightarrow n$, $p \leftrightarrow r$, $q \leftrightarrow s$. This is consistent with power conservation, which in the absence of significant ohmic loss requires

$$K_{nm} = -K_{mn}^*. \quad \text{(A25)}$$

In the present case, all the K_{mn} are real. A separate derivation of the coupling factor for coupling from $\mathrm{TM}_{pq}(m)$ to $\mathrm{TE}_{rs}(n)$ demonstrates that (A25) holds for the K_{mn} in (A24) also.

For the simplest coupling, from TE_{10} to TE_{01},

$$K_{mn} = \frac{(P_m + P_n)}{(P_m P_n)^{1/2}} \frac{K_0 \theta'}{2}, \qquad \mathrm{TE}_{10}\text{–}\mathrm{TE}_{01}. \quad \text{(A26)}$$

When both modes are far above cutoff, P_m and P_n both approach unity, and $K_{mn} \equiv K_0 \theta'$, which is independent both of waveguide size and of frequency. Similar situations hold for twist coupling between other modes (see Table I).

For comparison with other work, we note that (A26) agrees with the result of Katsenelenbaum [3], who derived the twist coupling between these two modes only.

Marhic [4] derived the twist coupling factors between any two modes, assuming that they were all far from cutoff. However, in his result for TE_{pq} to TE_{rs} coupling, the normalization factors $\epsilon_m = 2$ and $\epsilon_n = 2$ for TE_{p0} or TE_{0s} modes are missing. Furthermore, he obtains no coupling at all between two TM modes. Otherwise, Marhic's results agree with (A17) and (A24).

An alternative derivation of the coupling coefficients may use the generalized telegraphist's equation approach [13]. In this approach, Maxwell's equations are converted to the form

$$\frac{dV_m}{dz} = T_{mm} V_m + \sum_{n \neq m} T_{nm} V_n - j\beta_m Z_m I_m \quad \text{(A27a)}$$

$$\frac{dI_m}{dz} = -T_{mm}^* I_m - \sum_{n \neq m} T_{mn}^* I_n - j\beta_m V_m / Z_m \quad \text{(A27b)}$$

where the Z_m are the modal wave impedances

$$Z_m = Z_0 / P_m \qquad \text{(TE modes)} \quad \text{(A28a)}$$

$$Z_m = Z_0 P_m \qquad \text{(TM modes).} \quad \text{(A28b)}$$

Z_0 is the impedance of free space, and the T_{mn} can be written in terms of integrals over the waveguide cross section.

By defining the traveling wave amplitudes,

$$A_m^{\pm} \exp(\mp j\beta_m z) = Z_m^{-1/2}(V_m \pm Z_m I_m)/2 \quad \text{(A29)}$$

we find that (A27) can be written in the form of (A7) if we neglect reflections (we assume the β_m are independent of

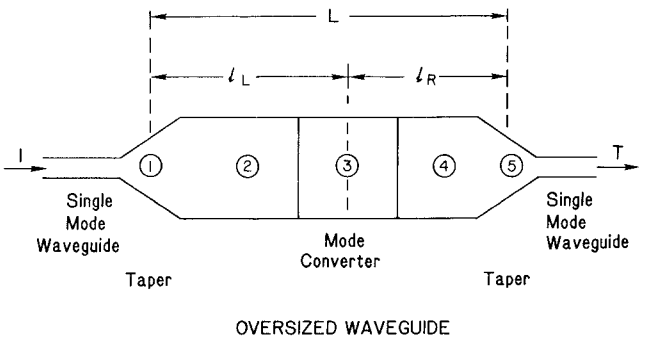

Fig. 10. Schematic of transmission through an overmoded waveguide with a mode converter that generates trapped modes.

z). The $A_m^{\pm}$ in (A29) are the same as in (A1), and the forward coupling coefficients $K_{mn}^{+} = K_{mn}$ are related to the T_{mn} in (A27) by

$$K_{mn} = \left[(Z_n/Z_m)^{1/2} T_{nm} - (Z_m/Z_n)^{1/2} T_{mn}^{*}\right]/2. \quad \text{(A30)}$$

We could also include reflections terms; to calculate the coupling coefficients K_{mn}^{-} for reflection, replace the minus sign in (A30) by a plus sign.

Now let us consider the relationship of the above results to those in Yabe and Mushiake [7]. When an incident mode $m = 1$ undergoes no reflections, we have $A_1^{+} = 1$ and $V_1/I_1 = Z_1$. Combining (A29) corresponding to $m = 1$ and $m = n$, we obtain

$$A_n^{\pm} = \left[(Z_1/Z_n)^{1/2} V_n \pm (Z_n/Z_1)^{1/2} I_n\right]/2 \quad \text{(A31)}$$

where

$$V_n \equiv V_n/V_1$$
$$I_n \equiv I_n/I_1. \quad \text{(A32)}$$

Let us identify $m = 1$ with TE_{10} and n with TE_{01}. V_n and I_n can then be obtained as the modal expansion coefficients for the dominant hybrid mode in a uniformly twisted rectangular waveguide. From Table 1 of Yabe and Mushiake's work [7], after some rewriting, we have

$$V_{01} = 2P_{10}^2 W$$
$$I_{01} = \left(P_{10}^2 + P_{01}^2\right) W \quad \text{(A33)}$$

where the normalized propagation constants P_{10} and P_{01} are as in (A13), and

$$W = -j(8/\pi^2)\theta'\left[kP_{10}\left(P_{10}^2 - P_{01}^2\right)\right]^{-1}. \quad \text{(A34)}$$

From (A28a) and (A31), we then have

$$A_{01}^{\pm} = -j\theta'(4/\pi^2)\left[(P_{10} \pm P_{01})/(P_{10} \mp P_{01})\right] \Big/ \left[k(P_{10}P_{01})^{1/2}\right]. \quad \text{(A35)}$$

In view of (3) and (A18), we find from (A35) that the forward coupled TE_{01} amplitude obtained from [7] is

$$A_{01}^{+} = -jK_{mn}/\Delta\beta_{mn} \quad \text{(A36)}$$

where K_{mn} is the forward coupling factor for TE_{10} to TE_{01} coupling given by (A26). The magnitude of the coupled TE_{01} mode calculated in this way agrees with the magnitude of forward coupled modes in uniformly coupled overmoded waveguides given by Unger [14]. Expressions for the amplitudes of the TE_{03}, TE_{21}, and TM_{21} modes could be obtained similarly from the modal expansion coefficients given in Yabe and Mushiake [7].

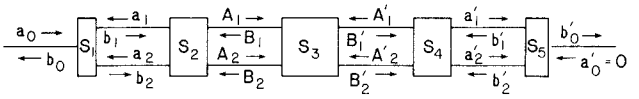

Fig. 11. Scattering matrices corresponding to the situation in Fig. 10.

Hence we have shown that deriving the coupling coefficients in the manner of this appendix is equivalent to the modal expression technique of [7].

Appendix II
Determination of Mode Conversion in an Overmoded Waveguide Component from Measurements of Resonance Loss in a Transmission Measurement Between Fundamental Waveguides

Consider the experimental situation shown schematically in Fig. 10. An oversized waveguide is connected at both ends by mode transducers and/or tapers to single-mode waveguide. A mode converter is located somewhere along the oversized waveguide, and we consider for the purposes of this analysis that the converter's effect is localized at a point.

Mathematically, we can model the arrangement in Fig. 10 by blocks $i = 1$ through 5 in Fig. 11, each with scattering matrix S_i. If we assume that the mode transducers and tapers connecting the single-mode and oversided waveguides are ideal, then there is no mode conversion or reflection associated with S_1 or S_5. The case where mode conversion does occur at both of these points was considered by King and Marcatili [15]; they did not consider a single mode converter located somewhere along the oversized waveguide. Klinger [16] refined this analysis for the case where an oversized waveguide is terminated in a short; the unfolded schematic shown in Figs. 10 and 11 (without the mode converter at $i = 3$) then can be used provided that S_1 and S_5 both represent the same mode transducer/taper under test. In any case, our assumption of ideal mode transducers/tapers can be checked experimentally prior to the insertion of the mode converter at $i = 3$ by checking that there are no significant resonances.

For ideal mode transducers/tapers, we have

$$S_1 = S_5 = \begin{bmatrix} 0 & 1 & 0 \\ 1 & 0 & 0 \\ 0 & 0 & 1 \end{bmatrix} \quad \text{(A37)}$$

$$[b_m] = S_1[a_m] \quad \text{(A38)}$$

and

$$[b_m'] = S_5[a_m'] \quad \text{(A39)}$$

where the matrices represented in brackets are column

matrices

$$[a_m] \equiv \begin{bmatrix} a_0 \\ a_1 \\ a_2 \end{bmatrix}, \quad \text{etc.} \tag{A40}$$

The blocks $i=2$ and $i=4$ represent lengths l_L and l_R, respectively, of ideal oversized waveguide; thus at $i=2$,

$$\begin{bmatrix} A_1 \\ a_1 \\ A_2 \\ a_2 \end{bmatrix} = \begin{bmatrix} 0 & e^{-j\phi_1} & 0 & 0 \\ e^{-j\phi_1} & 0 & 0 & 0 \\ 0 & 0 & 0 & e^{-j\phi_2} \\ 0 & 0 & e^{-j\phi_2} & 0 \end{bmatrix} \begin{bmatrix} B_1 \\ b_1 \\ B_2 \\ b_2 \end{bmatrix} \tag{A41}$$

where

$$j\phi_n = \Gamma_n l_L, \qquad n=1,2 \tag{A42}$$

represent the propagation factors of the desired ($n=1$) and unwanted ($n=2$) modes, respectively. The situation at $i=4$ is the same, except that all the elements in the matrices of (A41) are replaced by primes, and

$$j\phi_n = \Gamma_n l_R, \qquad n=1,2. \tag{A43}$$

Finally, at the mode converter $i=3$ we have

$$\begin{bmatrix} B_1 \\ B_1' \\ B_2 \\ B_2' \end{bmatrix} = \begin{bmatrix} 0 & T_0 & T_1 & T_2 \\ T_0 & 0 & T_3 & T_1 \\ T_1 & T_3 & 0 & T_4 \\ T_2 & T_1 & T_4 & 0 \end{bmatrix} \begin{bmatrix} A_1 \\ A_1' \\ A_2 \\ A_2' \end{bmatrix}. \tag{A44}$$

Here we have assumed that the converter is symmetric and also does not generate reflections. Far above cutoff in oversized waveguide, the reflections are ordinarily totally negligible. We accordingly also neglect reflection coupling between modes:

$$T_1 = 0. \tag{A45}$$

Further, from the requirement of power conservation in a mode converter with no ohmic dissipation, we have

$$T_3 = -T_2^* \tag{A46}$$

(compare the analogous statement in (4)),

$$T_0 = T_4^* \tag{A47}$$

(see the perturbation solutions (119)–(120) of Rowe and Warters [17]), and finally

$$|T_0|^2 = 1 - |T_2|^2 \tag{A48}$$

(see Fig. 11).

To solve for the transmission

$$T \equiv b_0'/a_0 \tag{A49}$$

we first solve successively for b_0' in terms of a_1', B_1', A_1 and A_2, b_1 and b_2, and finally a_0 and a_2 by working to the left in Fig. 11 using (A37), (A41), and (A44). Then a_2 is written in terms of a_2' by working to the right in Fig. 11 ($a_0'=0$), and a_2' is in turn written in terms of a_0 and a_2 by working to the left. Hence a_2 can be solved in terms of a_0 alone, and substitution in the expression for b_0' previously discussed yields b_0' in terms of a_0 as desired. If we write

$$|T| \equiv e^{-\alpha_1 L}|T_0||F| \tag{A50}$$

where

$$L = l_L + l_R \tag{A51}$$

$\alpha_1 L$ being the one-way attenuation of the desired mode and the quantity F describing the resonance behavior, then

$$\frac{|F|^2_{\min}}{|F|^2_{\max}} = \frac{1 - \dfrac{2|T_2|^2 E}{1+E}}{1 + \dfrac{2|T_2|^2 E}{1-E}} \tag{A52}$$

where

$$E = \exp(-\alpha_2 L) \tag{A53}$$

represents the one-way attenuation of the unwanted mode. In deriving (A52), we have assumed that $|T_2|^2 \ll 1$. ($|T_2|^2$ is the relative power converted to the unwanted mode in one pass of the mode converter when all of the power is initially in the desired mode.)

Note that if there is little ohmic loss for the unwanted mode, the resonances can become very deep. In fact, in the limit of $\alpha_2 = 0$, $E=1$, $|F|^2_{\min}$ goes to zero for all values of $|T_2|^2$. When $\alpha_2 L$ is small, (A52) becomes approximately

$$\frac{|F|^2_{\min}}{|F|^2_{\max}} \cong \left(1 + \frac{|T_2|^2}{\alpha_2 L}\right)^{-1}, \qquad \alpha_2 L \ll 1. \tag{A54}$$

This highlights the importance of the ratio of the one-way mode converted power $|T_2|^2$ to the one-way attenuation of the unwanted mode.

The resonances where $F = F_{\min}$ occur at very fine intervals when the length L is large compared to the guide wavelength of the unwanted mode [15]. The resonance condition is

$$\beta_2 L = m\pi + \text{const}, \qquad m \text{ integer} \tag{A55}$$

where the complex propagation constants in (A42) are

$$\Gamma_n = \alpha_n + j\beta_n, \qquad n=1,2. \tag{A56}$$

If the length of oversized waveguide is very long, however, so that $\alpha_2 L$ becomes large with respect to unity, then $|F|^2_{\min}/|F|^2_{\max}$ also approaches unity, showing that the resonances have been smeared out. That is, the "Q" of the cavity in Fig. 11 has become very small.

To determine the mode conversion $|T_2|^2$ from a measurement of the loss resonances using (A52) or (A54) and (A53), the loss $\alpha_2 L$ of the unwanted mode in the oversized waveguide "cavity" must be known. If the loss $\alpha_1 L$ of the desired mode can be measured, and if the "cavity" length L is large enough that the losses in the oversized waveguide are large compared with the losses in the mode launchers and/or tapers at each end, then $\alpha_2 L$ can be estimated from $\alpha_1 L$ using the formulas for attenuation of various modes. Deviations from ideal surface resistivity should make the ratio of actual to theoretical attenuation the same for both modes.

Alternatively, the loss resonances can be compared with those of a "calibrated" mode converter. For example, the mode conversion from TE_{10} to TE_{01} in an abrupt twist of (small) angle change $\Delta\theta$ is just $|T_2| = K_0 \Delta\theta = (8/\pi^2)\Delta\theta$.

ACKNOWLEDGMENT

The author wishes to thank T. N. Anderson of Antennas for Communication, Inc. for stimulating much of this work and for supplying Fig. 8 and the data taken on that twist, which was developed for the Norden Systems Division of United Technologies, Inc. under contract with the Federal Aviation Administration.

REFERENCES

[1] J. L. Doane and T. N. Anderson, "Oversized rectangular waveguides with mode-free bends and twists for broadband applications," *Microwave J.*, to be published.

[2] J. P. Quine, "Oversize tubular metallic waveguides," in *Microwave Power Engineering*, vol. 1, E. C. Okress, Ed. New York: Academic Press, 1968, pp. 178–213.

[3] B. Z. Katsenelenbaum, *Theory of Nonuniform Waveguides with Slowly Varying Parameters*, Moscow: Izd. Akad Nauk SSSR, 1961 (in Russian).

[4] M. E. Marhic, "Loss increases in multimode rectangular infrared waveguides due to helical deformations," *IEEE Trans. Microwave Theory Tech.*, vol MTT-30, pp. 671–678, May 1982.

[5] J. W. Carlin and S. C. Moorthy, "TE_{01} transmission in waveguide with axial curvature," *Bell Syst. Tech. J.*, vol. 56, pp. 1849–1872, Dec. 1977.

[6] J. L. Doane, "Propagation and mode coupling in corrugated and smooth-wall circular waveguides," in *Infrared and Millimeter Waves*, vol. 13, K. J. Button, Ed. New York: Academic Press, 1985.

[7] H. Yabe and Y. Mushiake, "An analysis of a hybrid-mode in a twisted rectangular waveguide," *IEEE Trans. Microwave Theory Tech.*, vol. MTT-32, pp. 65–71, Jan. 1984.

[8] X. S. Fang and Z. Q. Lin, "A coupled-mode approach to the analysis of fields in space-curved and twisted waveguides," *IEEE Trans. Microwave Theory Tech.* vol. MTT-35, pp. 978–983, Nov. 1987.

[9] S. E. Miller, "Coupled wave theory and waveguide applications," *Bell Syst. Tech. J.*, vol. 33, pp. 661–720, May 1954.

[10] J. L. Doane, "Hyperbolic secant coupling in overmoded waveguide," *IEEE Trans. Microwave Theory Tech.*, vol. MTT-32, pp. 1362–1371, Oct. 1984.

[11] J. L. Doane, "Polarization converters for circular waveguide modes," *Int. J. Electron.*, vol. 61, pp. 1109–1133, Dec. 1986.

[12] H. C. Huang, "Generalized theory of coupled local normal modes in multi-wave guides," *Scientia Sinica*, vol. 9, pp 142–154, Jan. 1960.

[13] S. A. Schelkunoff, "Conversion of Maxwell's equations into generalized telegraphist's equations," *Bell Syst. Tech. J.*, vol. 34, pp. 995–1043, Sept. 1955.

[14] H. G. Unger, "Normal mode bends for circular electric waves," *Bell Syst. Tech. J.*, vol. 36, pp. 1292–1307, Sept. 1957.

[15] A. P. King and E. A. Marcatili, "Transmission loss due to resonance of loosely-coupled modes in a multi-mode system," *Bell Syst. Tech. J.*, vol. 35, pp. 899–906, July 1956.

[16] Y. Klinger, "The measurement of spurious modes in over-moded waveguides," in *Proc. IEE Convention on Long Distance Transmission by Waveguide*, vol. 106, part B, supplement B, pp. 89–93, Sept. 1959.

[17] H. E. Rowe and W. D. Warters, "Transmission in multimode waveguide with random imperfections," *Bell Syst. Tech. J.*, vol. 41, pp. 1031–1170, May 1962.

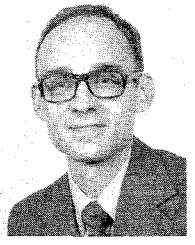

John L. Doane (S'66–M'66–SM'87) was born in New York City, N.Y, on June 20, 1942. He received the B.E. degree from Yale University, New Haven, CT, in 1964 and the Ph.D. degree from M.I.T., Cambridge, MA, in 1970.

From 1970 to 1977, he worked at Bell Laboratories, where he made measurements and analyses of mode conversion for long-distance millimeter waveguide communication systems, and worked on the design of an automated microwave transmission surveillance system. Since 1977, he has been designing millimeter-wave instrumentation and low-loss waveguide components for plasma diagnostics and heating at the Plasma Physics Laboratory of Princeton University, Princeton, NJ.